ADVANCED ENGINEERING MATERIALS
www.aem-journal.com

Mesoporous Silica Spheres Incorporated Aluminum/Poly (Vinylidene Fluoride) for Enhanced Burning Propellants

*Haiyang Wang, Jeffery B. DeLisio, Scott Holdren, Tao Wu, Yong Yang, Junkai Hu, and Michael R. Zachariah**

In this paper, we demonstrate that preparation by electrospray deposition of mesoporous SiO_2 particles can be employed as additives to Aluminum/Poly (Vinylidene Fluoride) (Al/PVDF) to enhance reaction velocity. We find that the reaction velocity of Al/PVDF with 5 wt% SiO_2 is 3× higher. The presence of meso-SiO_2 appears to accelerate the decomposition of PVDF, with a significant increase in HF release, resulting in higher heat release. We believe that hot-spots around meso-SiO_2 may serve as multiple ignition points, with the multi-layered structure promoting heat convection to increase the propagation rate.

1. Introduction

Due to its high energy density and availability, aluminum is commonly employed as a fuel in propellant systems. One key metric in energetic systems is burning rate, which can be tuned in various ways. For example, when replacing traditionally micro-sized aluminum particles with nano-sized counterparts, the burning rate of thermite systems can be increased by several orders of magnitude up to $\approx 1000\ m\ s^{-1}$.[1–3] This effect is caused by the reduced diffusion distances, increased interfacial contact area between the metal fuel and metal oxide oxidizer, and changes in modes of heat transfer.[4] In addition, additives such as ferrocene, iron oxide, and copper chromite particles have been found to increase burning rate of propellents.[5,6] These particles not only act as catalysts to lower the decomposition temperature of the oxidizer (e.g., ammonium perchlorate, AP),[7] but can also affect the thermal conductivity, in turn playing a role in binder melting (e.g., copper chromite in HTPB).[5] There are also physical methods to increase the burning rate such as the embedding of metal fibers into solid-propellant to increase the burning rate by increasing the thermal conductivity.[8–10] Oddly however, the burning rate of the solid-propellant has also been shown to increase when adding low thermal conductive materials such as silica and has never been fully explained.[11–13] Some suggest that silica disturbs the integrity of the propellant, creating pathways for oxygen diffusing to the surface of the metal.[11,14] Others have proposed that the heat conduction in the solid-propellant is obstructed by silica particles, and the area around the particles will have a much higher temperature owing to heat accumulation, resulting in formation of hot spots around the silica particles thus enhancing burning rate.[13]

To maximize energy density, high aluminum nanoparticles (Al NPs) loadings are desired, however, due to their high specific surface area and resultant high viscosity of the processing mix, creating a composite propellant with a homogeneous dispersion of high mass loading aluminum is highly challenging. Hydroxyl-terminated polybutadiene (HTPB), for example, is a commonly used binder in current propellant formulations owing to its superior mechanical properties with high loadings of metal particles. However, HTPB does not positively influence the energy density of the propellant and does not solve the issue of high viscosity during processing. Recently, fluoropolymers such as Polytetrafluoroethylene (PTFE, Teflon™)[15,16] have been shown to react exothermically with Al in addition to acting as a binder. More recently, Al NPs were dispersed into PVDF solution and directly electrosprayed to create free-standing high metal loading (50 wt%) Al/PVDF films.[17] However, these Al/fluoropolymers have slow burning rates. One intriguing result is that the alumina shell (Al_2O_3) from the Al shows a pre-ignition reaction with fluoropolymers.[15–18] Although it appears not to enhance the burning rate.[18]

In this paper, we investigate how additives in Al/PVDF can affect the thermal properties and reaction characteristics. Silica in different forms (nanosized, microsized, and mesoporous) were incorporated during electrospray fabrication into Al/PVDF films and the resulting morphologies, crystalline phases, thermal properties, and combustion characteristics were evaluated. The results show that with only a 5 wt% addition of mesoporous silica, the burning rate of Al/PVDF film was increased by a factor of three. Mesoporous silica was found to promote the decomposition of PVDF as well as create hot spots to accelerate reaction.

2. Experimental Section

2.1. Chemicals

Aluminum nanoparticles (Al NPs, ≈85 nm) were purchased from Novacentrix with an active aluminum content of ≈81 wt%.

Prof. M. R. Zachariah, Dr. H. Wang, Dr. J. B. DeLisio, S. Holdren, T. Wu, Y. Yang, Dr. J. Hu
Department of Chemical and Biomolecular Engineering and Department of Chemistry and Biochemistry, University of Maryland, College Park, MD 20742, USA
E-mail: mrz@umd.edu

DOI: 10.1002/adem.201700547

The poly-vinylidene fluoride (PVDF),[19–20] nano-sized silica (nano-SiO_2, ≈10–15 nm, as Figure S1 shows), and micro-sized silica (micro-SiO_2, ≈1–5 μm; see Figure S1) were purchased from Sigma-Aldrich. N, N-Dimethylformamide (DMF) was purchased from BDH chemicals. Colloidal silica (SNOWTEX ST-PS-S, 15–16 wt% SiO_2) was purchased from Nissan Chemical Industries, Ltd. All chemicals were used as received.

2.2. Spray Dry Formation of Mesoporous SiO_2 Particles

The as received SiO_2 colloidal solution is ≈10–15 nm. The mesoporous SiO_2 particles (meso-SiO_2) were produced by a "droplet-to-particle" aerosol spray dry process to yield meso-particles of average diameter of ≈0.9 μm (0.2–4 μm). The spray drying setup can be found in our previous studies.[21,22] The aerosol droplets were generated (≈1 μm) using compressed air at a pressure of 0.24 MPa in a collision-type atomizer, which passed through a silica-gel diffusion dryer to remove water, and then to a tube furnace at 300 °C. The products were collected on a 0.4 μm (pore size) Millipore filter. After the spray-drying, the product was collected in a glass vial and kept in an oven (≈100 °C) to avoid any moisture absorption. Scanning electron microscope (SEM) and transmission electron microscope (TEM) images of the formed mesoporous SiO_2 particles are shown in **Figure 1**. Thermogravimetry/Differential Scanning Calorimetry (TG/DSC) and Fourier Transform Infrared Spectroscopy (FTIR) results show ≈5 wt% of both physically adsorbed and structural water in the formed SiO_2 mesoparticles (Figure S2). As Figure S3 shows (Brunauer–Emmett–Teller test, BET test), the produced SiO_2 particles are mesoporous, with a specific surface area of 139 $m^2 g^{-1}$ and an average pore size of ≈15 nm. By comparison the purchased micro-SiO_2 show a specific surface area of ≈6 $m^2 g^{-1}$ with no porosity (Figure S3).

2.3. Electrospray Formation of Al/PVDF Films with and without SiO_2

The details about the electrospray system can be found in our previous studies.[17,18,23–27] PVDF powder was first dissolved into DMF to which Al NPs were added. Lastly, mesoporous SiO_2 particles were added into the Al/PVDF suspension. In a typical experiment, 150 mg PVDF was dissolved in 3 mL DMF, then 52.2 mg Al NPs and 10.6 mg SiO_2 particles were added. The final suspension was sonicated for 1 h and stirred for 24 h. The stirring process and electrospray was conducted in a fume hood which has an average temperature of ≈35 °C and an average humidity of 67%.

2.4. Reactive Chemistry and Structure Characterization

The produced Al/PVDF films (with and without SiO_2) were characterized using a Hitachi SU-70 scanning electron microscope (SEM) coupled to an energy dispersive spectrometer (EDS). The films were broken with tweezers in liquid nitrogen for cross-section imaging of the films. The mesoporous SiO_2 particle were also characterized by transmission electron microscopy (TEM) (JEOL 2100F field-emission instrument). The different SiO_2 particles were characterized by powder X-ray diffraction (XRD, Bruker D8 with Cu K radiation) and Fourier transform infrared spectroscopy (FTIR, Nicolet i550R, Thermo Fisher Scientific), respectively. Thermogravimetry/differential scanning calorimetry (TG/DSC) results were obtained with a TA Instruments Q600 in an argon or oxygen atmosphere (flow rate: 100 mL min^{-1}) coupled to a mass spectrometer with different heating rates (as labeled). The sample mass was ≈1.3–1.9 mg and the heat flow was normalized to mass.

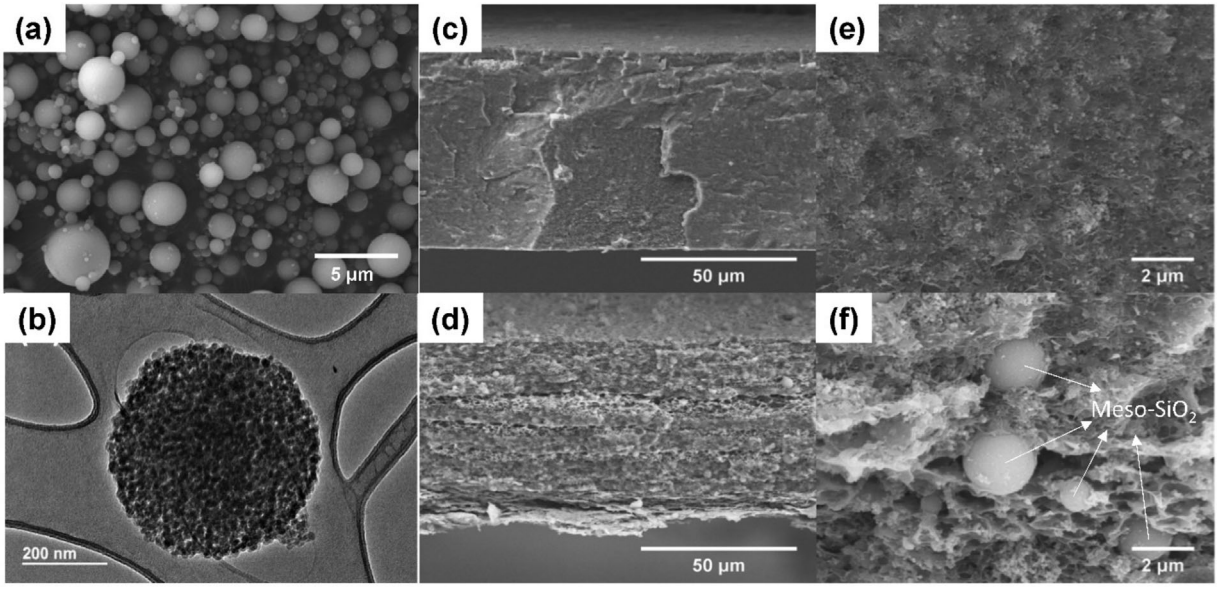

Figure 1. The SEM a) and TEM b) images of mesoporous silica (meso-SiO_2) prepared by spray-drying. Low c and d) and high e and f) resolution SEM images of Al-PVDF films without c and e) and with meso-SiO_2 films d and f).

T-Jump Time-of-Flight mass spectrometry (T-Jump TOFMS) was also used for characterizing the species released during fast heating. The details of the T-Jump time-resolved mass spectrometer system can be found in refs.[28,29] Typically, a ≈10 mm long platinum filament (≈76 μm in diameter) coated with the sample (≈4 mm long) was resistively heated to ≈1600 K (heating rate of $\approx 4 \times 10^5$ K s^{-1}). The sample was coated on the wire by direct electrospraying.[18] The precursor for preparing SiO_2/PVDF film had 150 mg PVDF and 150 mg SiO_2 in 3 mL DMF.

2.5. Burning Rate Measurements

The burning rate tests were conducted in a quartz tube filled with argon on 3 × 0.5 cm samples. The film was fixed on two parallel copper wires with tape to minimize any curling of the film during burning. The films were ignited by resistively heating a Nichrome wire (≈1 cm in length, 0.010 inches in diameter; TED PELLA. INC) triggered by an external DC power supply. After each run, the tube was cleaned and purged with a flow of argon for 5 min (10 L min^{-1}). The burning of the films was monitored using a high-speed camera (14.9 μs per frame with 256 × 256 pixels, Phantom V12.1). Each sample was tested three times and the average values with standard deviation are reported.

2.6. Combustion Cell Measurements

The details of the combustion cell experiment can be found in our previous studies.[26,27] The gas generating ability of the Al/PVDF films (with and without meso-SiO_2) was evaluated in a constant volume (≈20 cm^3) combustion cell, from which the pressure and optical emission histories can be simultaneously obtained. The sample mass was ≈25 mg, and experiments were replicated in triplicate.

3. Results and Discussion

3.1. The Effect of Different SiO_2 on the Morphology of Al/PVDF Films

Al/PVDF films with (5 wt%) and without meso-SiO_2 were prepared by electrospray deposition. The SEM and TEM images of mesoporous silica, the SEM images and EDS results (EDS results are shown in Figure S4) of the two Al/PVDF films are shown in Figure 1. As Figure 1c and e show, the Al/PVDF films without meso-SiO_2 are dense with a homogenous dispersion of Al NPs in the PVDF matrix (Figure S4d). In contrast, with 5 wt% meso-SiO_2 particles, the formed films show a multi-layered structure (Figure 1d and f). For comparison, Al/PVDF films with nano-SiO_2 and micro-SiO_2 were also prepared by the same procedure, as shown in Figure S5. Both cases show dense films, especially for the case with micro-SiO_2, (Figure S5d). One interesting fact for the case with nano-SiO_2 is that nano-SiO_2 particles were well dispersed in the precursor after sonication and were found to coat the surface of the Al NPs (Figure S5b). Importantly,we note that the meso-SiO_2 spheres retain their integrity during the preparation process, as shown in Figure 1f and Figure S4d.

3.2. The Effect of Different Forms of SiO_2 on the Crystalline Phase of PVDF Films

The obvious changes to the structure of the films with the addition of meso-SiO_2 suggest that there may be significant interaction between PVDF and SiO_2.[19,20] To evaluate this, films at 50 wt% silica loading with micro-SiO_2, nano-SiO_2, and meso-SiO_2 were prepared and characterized by XRD and FTIR. FTIR results in **Figure 2**a show that the signatures for the α-phase are all but gone in the for the meso-SiO_2-PVDF case relative to the neat PVDF. Silica addition in general seems to decrease the α-phase but appears to be most promoted with the meso particle.

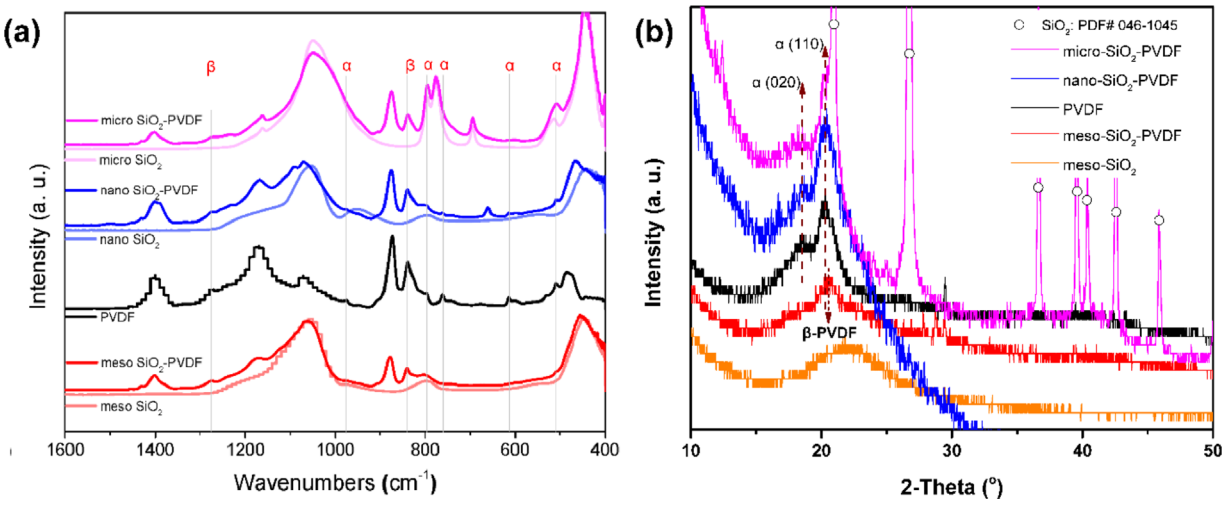

Figure 2. FTIR a) and XRD b) results of PVDF films with different SiO_2 particles and without SiO_2.

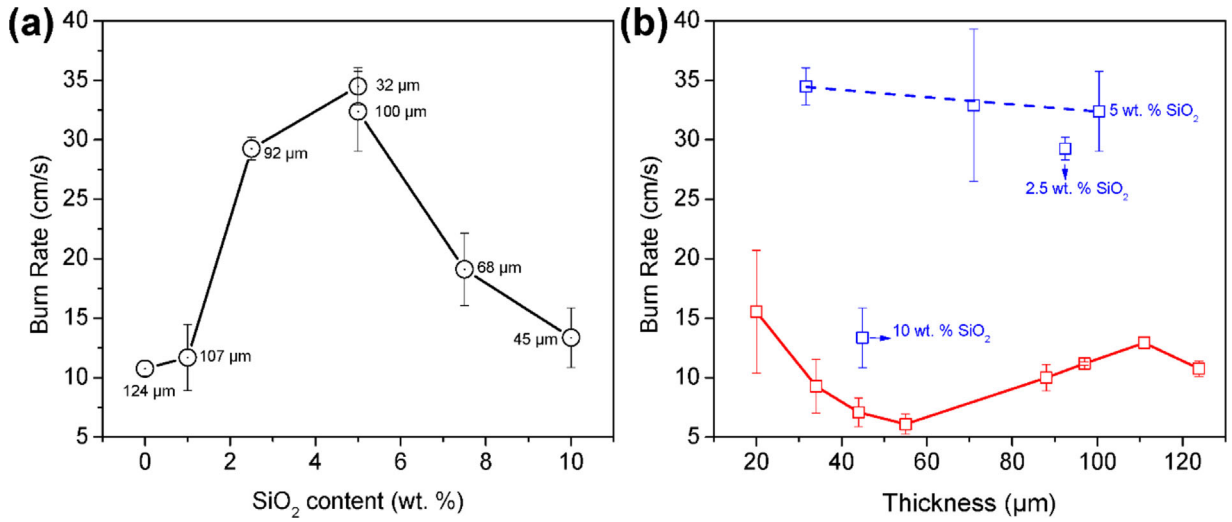

Figure 3. Burning rates of different Al/PVDF films with different meso-SiO_2 contents a) and different thicknesses (b), with 5 wt% SiO_2, blue dash line; without SiO_2, red line). Labeled are the thicknesses of different films. SiO_2 particles here are mesoporous except otherwise noted.

XRD which because of low crystallinity has poor signal to noise, and thus less convincing, indicates similar behavior in Figure 2b with a disappearance of the α-phase peak at 18°. Using formulations employed for our burning measurements Al/PVDF films with and without 5 wt% meso-SiO_2 (Figure 1) we still see that addition of meso-silica triggers the β-phase (Figure S6).

3.3. The Effect of Meso-SiO_2 on the Burning Rate of Al/PVDF Films

The burning rates of Al/PVDF films with different meso-SiO_2 content were measured in triplicate in an argon atmosphere. **Figure 3**a shows that with increasing meso-SiO_2 content, the burning rate increases by up to a factor of three at ≈5 wt% and then declines with increasing meso silica content. For comparison, Al/PVDF films with 5 wt% nano-SiO_2 (≈50 μm) and micro-SiO_2 (≈70 μm) were found to be only marginally higher.

The effect of film thickness on propagation velocity is shown in Figure 3b. Meso-silica added material has essentially film thickness independent while the Al/PVDF alone films do show some thickness dependence but is consistently and significantly below that of the meso particle added material. The apparent trend seen in the Al/PVDF films is probably a reflection of the larger error bars for the thin films rather than any underlying thickness dependence.

3.4. The Effect of Meso-SiO_2 on the Flame Structure

The burning of the Al/PVDF films with and without meso-SiO_2 were recorded with a high-speed camera and the corresponding snapshots are shown in **Figure 4**. In addition to the obvious faster burning rate, the meso-SiO_2 containing case has a much larger and brighter flame. Moreover, the size and shape of the flames in the two cases is also dissimilar. The flame size and shape for the case of no meso-SiO_2 remains small and constant during the whole process, while for the meso-SiO_2 case, the higher volume presumably provided great radiative heat feedback. The burning residues for the two cases are also very different. The burn residues for Al/PVDF with no SiO_2 remain as an intact structure, while those with 5 wt% SiO_2 were ejected along with the propagating flame.

3.5. The Effect of Meso-SiO_2 on the Reactivity of Al/PVDF Films

To measure the gas generating properties and reactivity of Al/PVDF films with (5 wt%) and without meso-SiO_2, ≈25 mg of film (size: 0.5 × 0.5 cm) was ignited in a confined combustion cell (≈20 mL) while the pressure and optical emission histories were simultaneously obtained. Three runs were conducted for each sample, and the average with standard deviation are reported. The detailed data including peak pressures, pressure rise rates and burn times was shown in Table S1, and the typical pressure and optical emission histories were shown in **Figure 5**. As Figure 5a and Table S1 shows, the average peak pressure and pressurization rate of 5 wt% meso-SiO_2 containing Al/PVDF films are ≈206 and ≈38 kPa ms^{-1}, which are ≈1.5 and 10.8 times higher than that of Al/PVDF without SiO_2, respectively. The high gas generating ability is consistent with the large flame volume observed in the burning rate measurements (Figure 4) and further confirm that meso-SiO_2 containing Al/PVDF films has higher reactivity.

3.6. The Effect of Different SiO_2 on the Thermal Decomposition of PVDF at Low Heating Rate

The role of silica in promoting the decomposition of PVDF was evaluated at low and high heating rates, with TG/DSC and

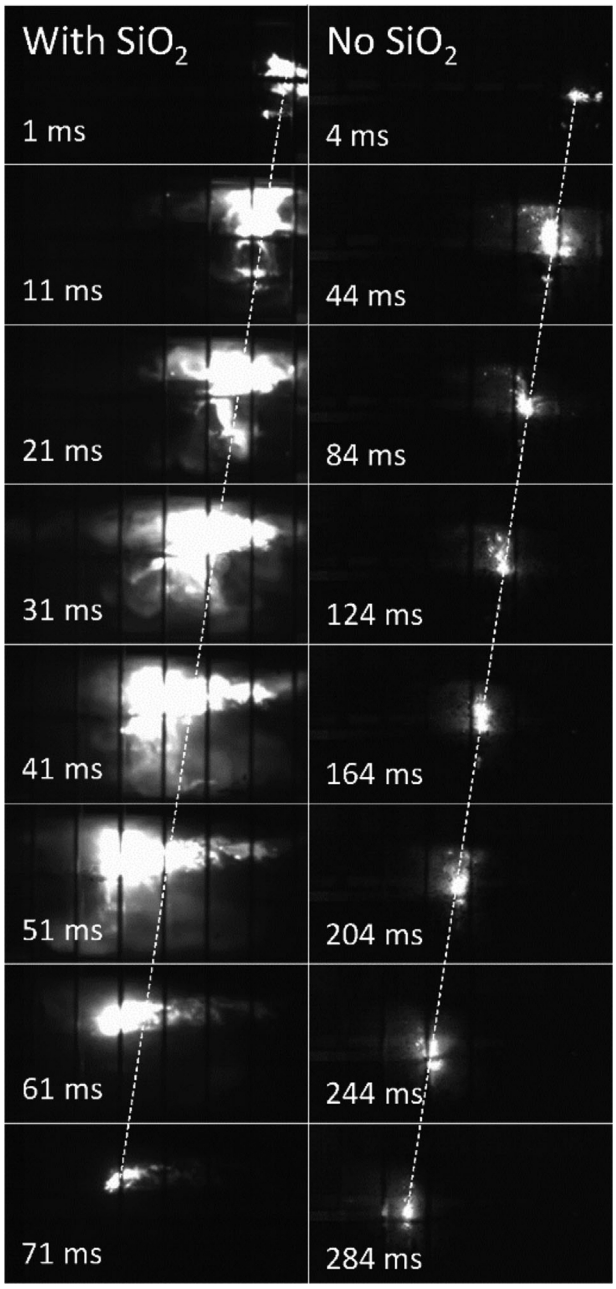

Figure 4. Snapshots of burning Al/PVDF films with (5 wt%) and without meso-SiO_2.

T-Jump TOFMS, respectively. Slow heating TG/DSC in argon environments are frequently employed to investigate the thermal behavior of Al and fluoropolymers.[17,18,30,31] However, as our previous study showed, the PVDF decomposition endotherm overlaps the early exotherm between alumina and PVDF.[18] Therefore, the TG/DSC of pure PVDF and PVDF/SiO_2 (1:1, by mass) films were run under 100 mL min^{-1} of pure oxygen at heating rates of 25 °C min^{-1}, and the TG and DSC results shown in **Figure 6**a and b, repectively.[31] The oxidation of PVDF in O_2 is exothermic, with the onset temperature close to the decomposition temperatures of PVDF. As Figure 6b shows, for pure PVDF, the DSC curve clearly shows three exotherms for decomposition and oxidation with a wide temperature range from 400 to 550 °C.

In contrast addition of silica changes dramatically both the oxidation kinetics as well as the heat release profile to that of one narrow exotherm over a small temperature range. The onset temperature appears to depend on the form of silica added with meso having the lowest onset and the micron the highest. The acceleration of the chemistry with silica addition, and in particular with the meso-silica is best seen in the TGA which shows a very dramatic reaction rate increase. T-Jump (heating rate of $\approx 4 \times 10^5$ K s^{-1}) mass spectrometry of pure PVDF and meso-SiO_2/PVDF show clearly the formation of SiF_3^+ (Figure S7) and an enhanced release of HF. The final weight loss of PVDF/silica after heating in TGA is higher than 50 wt% (Figure S8). Indicating a clear chemical interaction with silica and implying the effects seen are more than simply a physical effect.

3.7. The Effect of Meso-SiO_2 on the Heat Release of Al/PVDF at Low Heating Rate

The exothermic properties of Al/PVDF films with (5 wt%) and without SiO_2 particles were also investigated by DSC at heating rates of 5, 20, and 50 °C min^{-1} in an argon atmosphere. The corresponding TG/MS was employed to evaluate the relative HF released during decomposition (20 °C min^{-1}). As **Figure 7**a shows, under different heating rates, the integrated heat release from Al/PVDF/SiO_2 (5 wt%) films are all considerably higher than that from neat Al/PVDF films (3.3–1.2 higher depending on heating rate). As Figure 7b shows, the normalized HF intensity (normalized to 114, $C_3F_4H_2$) from Al/PVDF/SiO_2 (5 wt%) is also much higher than that from Al/PVDF case. The results indicate that with SiO_2 catalysis, PVDF will decompose much more completely and rapidly, releasing more HF gas to react with Al to produce more heat.

3.8. Proposed Mechanism

We observe that the thermal decomposition of PVDF is promoted by the addition of meso-SiO_2 particles fabricated by electrospray. We find that with only an addition of 5 wt% meso-SiO_2, the heat release from Al/PVDF film was significantly increased, resulting in much larger and brighter flame. We also observe a temporally enhanced HF release. The latter point suggests a chemical interaction although a physical effect may also play a role, given that nano-silica does not have a significant effect. It is possible that as schematically represented in **Figure 8** that the low thermal conductivity of mesoporous SiO_2 particles will act as heat transfer barrier producing hot-spots for multi-ignition points.[13] Perhaps more importantly, upon ignition, the hot particles/gas products will be ejected by the released high-pressure gas to increase the size of the flame and promote radiative feedback and convective heat transfer.[4]

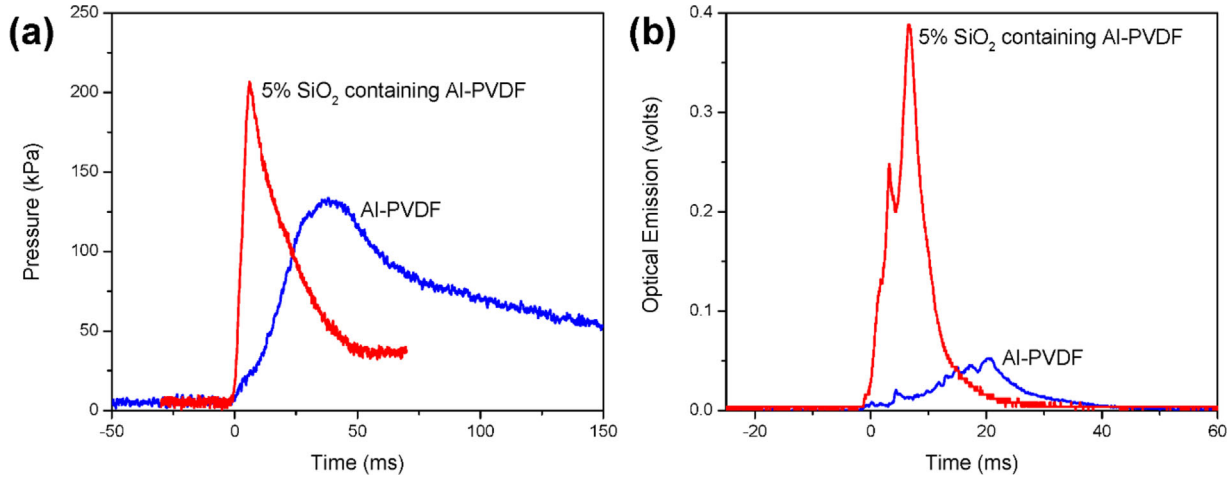

Figure 5. The pressure a) and optical emission b) histories of Al/PVDF films with (5 wt%, red line) and without SiO_2 (blue line).

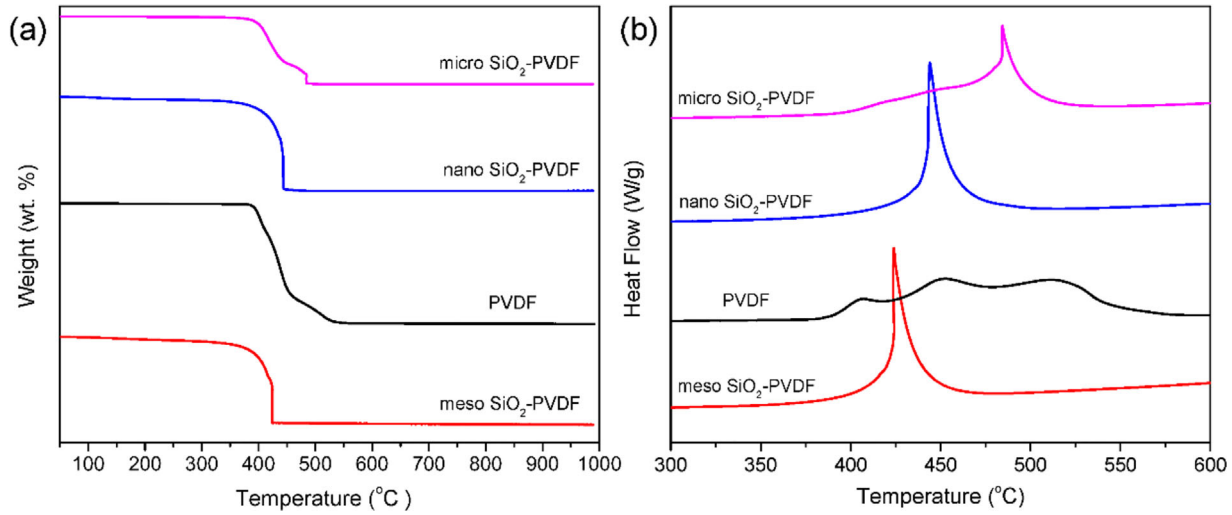

Figure 6. TGA a) and DSC b) results for PVDF films with (50 wt%) and without SiO_2.

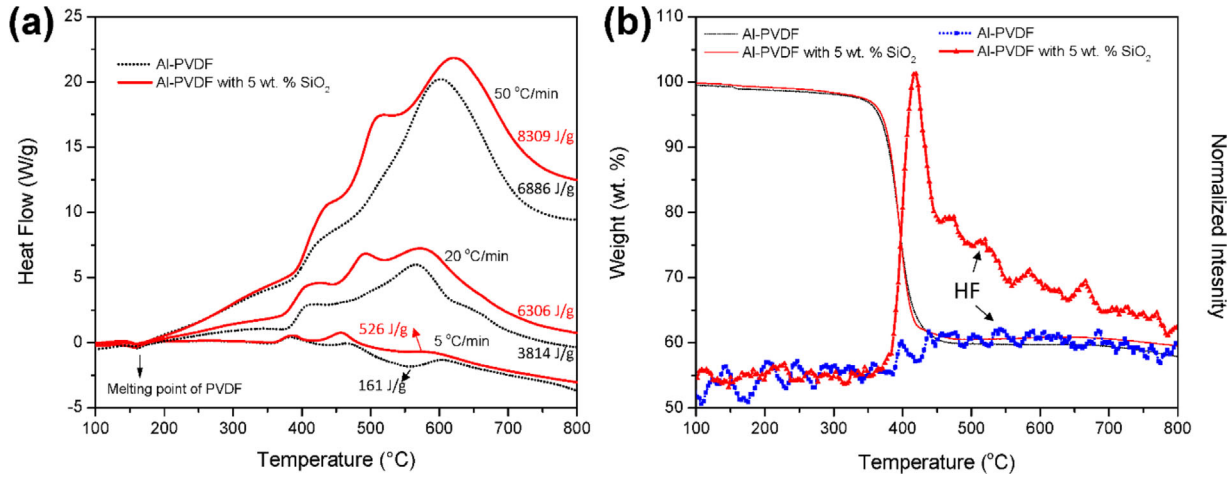

Figure 7. DSC a), TG and MS results b) of Al/PVDF films and Al/PVDF/SiO_2 (5 wt%) films. Note: the calculated exothermic energy is integrated from 200 to 800 °C. The intensity of HF ($m/z = 20$) was normalized based on argon ($m/z = 40$).

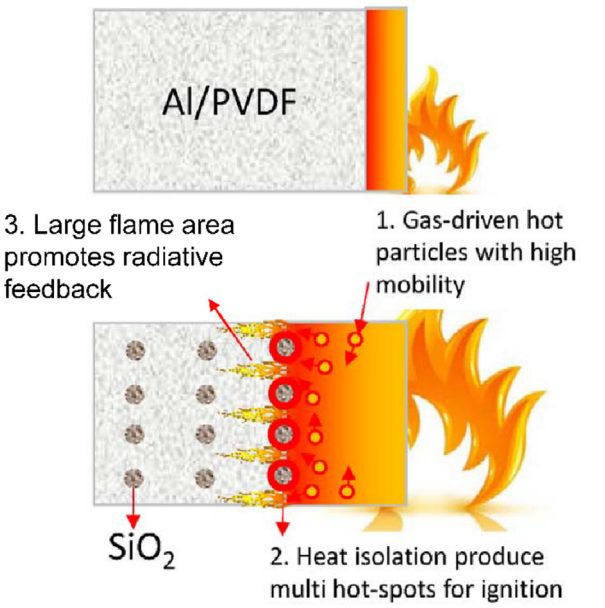

Figure 8. Possible mechanism for enhanced burning of Al/PVDF films by SiO_2 mesoparticles.

4. Conclusions

In this study, mesoporous SiO_2 particles were prepared using spraying drying process and were added into Al/PVDF films as a burning rate modifier. The burning rates of different Al/PVDF films with and without meso-SiO_2 particles were measured. The results show that the addition of SiO_2 mesoparticles (5 wt% SiO_2), enhanced the burning by $>3\times$. The presence of meso-SiO_2 appears to highly accelerate the decomposition of PVDF, with a significant increase in HF release and resulting in higher heat release. We also believe that hot-spots around meso-SiO_2 may help to serve as multiple ignition points and the multi-layered structure promote the heat convection thus highly increase the flame spreading rate.

Supporting Information

Supporting Information is available from the Wiley Online library or from the author.

Acknowledgements

This work was supported by DTRA and AFOSR. We acknowledge the support of the Maryland Nanocenter and its NispLab. The NispLab is supported in part by the NSF as a MRSEC Shared Experimental Facility.

Conflict of Interest

The authors declare no conflict of interest.

Keywords

aluminum, burning rate, films PVDF, mesoporous silica particles

Received: June 27, 2017
Revised: October 2, 2017
Published online: November 14, 2017

[1] G. C. Egan, K. T. Sullivan, T. Y. Olson, T. Y. Han, M. A. Worsley, M. R. Zachariah, *J. Phys. Chem. C* **2016**, *120*, 29023.
[2] M. L. Pantoya, J. J. Granier, *Propellants Explos. Pyrotech.* **2005**, *30*, 53.
[3] E. L. Dreizin, *Prog. Energy Combust. Sci.* **2009**, *35*, 141.
[4] G. C. Egan, M. R. Zachariah, *Combust Flame.* **2015**, *162*, 2959.
[5] K. Ishitha, P. A. Ramakrishna, *Combust. Flame* **2014**, *161*, 2717.
[6] M. A. Stephens, E. L. Petersen, D. L. Reid, R. Carro, S. Seal, *J. Propul. Power* **2009**, *25*, 1068.
[7] H. Wang, R. Jacob, J. Delisio, *Combust Flame*, **2017**, *180*, 175.
[8] L. H. Caveny, R. L. Glick, L. H. Caveny, R. L. Glick, L. H. Caveny, R. L. Glick, *J. Spacecraft Rockets* **1967**, *4*, 79.
[9] S. Isert, C. D. Lane, I. E. Gunduz, S. F. Son, *Proc. Combust. Inst.* **2017**, *36*, 2283.
[10] X. Li, M. R. Zachariah, *Propellants Explos. Pyrotech.* **2017**, *9*, 1079.
[11] L. D. Romodanova, P. K. Pokhil, *Combust. Explos. Shock Waves* **1970**, *6*, 258.
[12] J. L. Sabourin, R. A. Yetter, B. W. Asay, J. M. Lloyd, V. E. Sanders, G. A. Risha, S. F. Son, *Propellants Explos. Pyrotech.* **2009**, *34*, 385.
[13] S. Shioya, M. Kohga, T. Naya, *Combust. Flame* **2014**, *161*, 620.
[14] R. Chen, Y. Luo, J. Sun, G. Li, *Propellants Explos. Pyrotech.* **2012**, *37*, 422.
[15] K. Kappagantula, M. L. Pantoya, *Int. J. Heat Mass Transfer* **2012**, *55*, 817.
[16] X. Zheng, A. D. Curtis, W. L. Shaw, D. D. Dlott, *J. Phys. Chem. C* **2013**, *117*, 4866.
[17] C. Huang, G. Jian, J. B. DeLisio, H. Wang, M. R. Zachariah, *Adv. Eng. Mater.* **2015**, *17*, 95.
[18] J. B. DeLisio, X. Hu, T. Wu, G. C. Egan, G. Young, M. R. Zachariah, *J. Phys. Chem. B* **2016**, *120*, 5534.
[19] L. Li, M. Zhang, M. Rong, W. Ruan, *RSC Adv.* **2014**, *4*, 3938.
[20] D. Yuan, Z. Li, W. Thitsartarn, X. Fan, J. Sun, H. Li, C. He, *J. Mater. Chem. C.* **2015**, *3*, 3708.
[21] X. Wang, T. Wu, M. R. Zachariah, *J. Phys. Chem. C.* **2017**, *121*, 147.
[22] T. Wu, A. SyBing, X. Wang, M. R. Zachariah, *J. Mater. Res.* **2017**, *32*, 890.
[23] X. Li, P. Guerieri, W. Zhou, C. Huang, M. R. Zachariah, *ACS Appl. Mater. Interfaces* **2015**, *7*, 9103.
[24] X. Hu, J. B. DeLisio, X. Li, W. Zhou, M. R. Zachariah, *Adv. Eng. Mater.* **2016**, *1*, 1500532. DOI: 10.1002/adem.201500532.
[25] H. Wang, G. Jian, S. Yan, J. B. DeLisio, C. Huang, M. R. Zachariah, *ACS Appl. Mater. Interfaces* **2013**, *5*, 6797.
[26] H. Wang, J. B. DeLisio, G. Jian, W. Zhou, M. R. Zachariah, *Combust. Flame* **2015**, *162*, 2823.
[27] H. Wang, G. Jian, W. Zhou, J. B. DeLisio, V. T. Lee, M. R. Zachariah, *ACS Appl. Mater. Interfaces* **2015**, *7*, 17363.
[28] L. Zhou, N. Piekiel, S. Chowdhury, M. R. Zachariah, *Rapid Commun. Mass Spectrom.* **2009**, *23*, 194.
[29] L. Zhou, N. Piekiel, S. Chowdhury, M. R. Zachariah, *J. Phys. Chem. C.* **2010**, *114*, 14269.
[30] J. Wang, Z. Qiao, Y. Yang, J. Shen, Z. Long, Z. Li, X. Cui, G. Yang, *Chem. Eur. J.* **2016**, *22*, 279.
[31] M. A. Hobosyan, K. G. Kirakosyan, S. L. Kharatyan, K. S. Martirosyan, *J. Therm. Anal. Calorim.* **2015**, *119*, 245.

